



UNIVERSITY OF LEEDS

This is a repository copy of *Scaling of Dzyaloshinskii-Moriya interaction with magnetization in Pt/Co(Fe)B/Ir multilayers*.

White Rose Research Online URL for this paper:
<https://eprints.whiterose.ac.uk/180627/>

Version: Accepted Version

Article:

Alshammari, K, Haltz, E, Alyami, M et al. (5 more authors) (Accepted: 2021) Scaling of Dzyaloshinskii-Moriya interaction with magnetization in Pt/Co(Fe)B/Ir multilayers. *Physical Review B: Condensed Matter and Materials Physics*. ISSN 1098-0121 (In Press)

This paper is protected by copyright. This is an author produced version of an article accepted for publication in *Physical Review B: Condensed Matter and Materials Physics*. Uploaded in accordance with the publisher's self-archiving policy.

Reuse

Items deposited in White Rose Research Online are protected by copyright, with all rights reserved unless indicated otherwise. They may be downloaded and/or printed for private study, or other acts as permitted by national copyright laws. The publisher or other rights holders may allow further reproduction and re-use of the full text version. This is indicated by the licence information on the White Rose Research Online record for the item.

Takedown

If you consider content in White Rose Research Online to be in breach of UK law, please notify us by emailing eprints@whiterose.ac.uk including the URL of the record and the reason for the withdrawal request.



eprints@whiterose.ac.uk
<https://eprints.whiterose.ac.uk/>

Scaling of the Dzyaloshinskii-Moriya interaction with magnetization in Pt/Co(Fe)B/Ir multilayers

Khulaif Alshammari,^{1,2} Eloi Haltz,¹ Mohammed Alyami,^{1,3} Mannan Ali,¹ Paul S. Keatley,⁴ Christopher H. Marrows,¹ Joseph Barker,¹ and Thomas A. Moore¹

¹*School of Physics and Astronomy, University of Leeds, Leeds, LS2 9JT, United Kingdom*

²*Physics Department, College of Science, Jouf University, P.O. Box 2014, Sakaka, 42421, Saudi Arabia*

³*Department of Physics, College of Science and Humanities in Al-Kharj,*

Prince Sattam bin Abdulaziz University, Al-Kharj 11942, Saudi Arabia

⁴*Department of Physics and Astronomy, University of Exeter, Exeter, EX4 4QL, United Kingdom*

Magnetic multilayers with perpendicular anisotropy and an interfacial Dzyaloshinskii-Moriya interaction contain chiral domain walls and skyrmions that are promising for applications. Here we measure the temperature dependence of the Dzyaloshinskii-Moriya interaction (DMI) in Pt/CoFeB/Ir and Pt/CoB/Ir multilayers by means of static domain imaging. First, the temperature dependences of saturation magnetization (M_S), exchange stiffness (A) and intrinsic perpendicular anisotropy (K_u) are determined. Then the demagnetized domain pattern in each multilayer is imaged by wide-field Kerr microscopy in the temperature range 9-290 K, and the characteristic domain period at each temperature is determined. We calculate the DMI constant D from an analytical expression for the domain wall energy density that treats the multilayer as a uniform medium. Scaling laws for K_u and D with the magnetization are established from the experiments. While the scaling of K_u is consistent with Callen-Callen theory, we find that the scaling of D is similar to that of A predicted theoretically (~ 1.8).

I. INTRODUCTION

In magnetic multilayers the interfacial Dzyaloshinskii-Moriya interaction (DMI)¹ causes domain walls to have a chiral spin structure, and if it exceeds a critical value, skyrmions can be stabilised². Even larger values of DMI produce spin spirals. The different chiral spin textures are stable only in quite limited regions of a parameter space where DMI, anisotropy, exchange stiffness and demagnetizing fields compete with each other. All of these energies are also temperature dependent. Chiral spin textures have been put forward for use in new types of magnetic memories, sensors and computing devices³. Many proposed devices use electric current to drive domain walls or skyrmions along narrow magnetic strips. The induced Joule heating will raise the temperature of the devices. Moreover, electronic devices are expected to operate over a range of temperatures around room temperature. It is therefore important to understand the temperature dependence of the different energy contributions. The changes in anisotropy, exchange stiffness and demagnetizing fields with temperature are reasonably well understood but the DMI less so. It is therefore important to measure the temperature dependence of DMI in a variety of candidate materials to improve understanding.

There is also a fundamental interest, because the temperature dependence can lead to a better understanding of the microscopic origin of the DMI in magnetic multilayers. However, there is as yet little agreement between the results. Anisotropy decreases with increasing temperature in a power law $K_u(T)/K_u(T=0) = m(T)^{l(l+1)/2}$, where $m = M_S(T)/M_S(0)$, the reduced magnetization, and l is the order of the anisotropy. This result is derived from Callen-Callen theory^{4,5}. There is not such a simple theory for the temperature dependence of the exchange stiffness or of the DMI but numerical simulations suggest that they also follow power laws $A(T)/A(T=0) = m(T)^\alpha$ and $D(T)/D(T=0) = m(T)^\delta$ and that the exponents α and δ are the same⁶⁻⁸.

While these works calculated $\alpha = 1.5$, the important conclusion that should be drawn from them is that $\alpha = \delta$. In general the value of the exponent will vary depending on the choice of lattice. One experimental study on Pt/Co/Cu superlattices⁹ finds $D(m) \sim m^{4.9}$, while another on [Pt/CoFeB/Ru]₂¹⁰ measures $D(m) \sim m^{1.86}$. So far it is not clear why such different values have been found.

Here we measure the temperature dependence $D(T)$ of the DMI in Pt/FM/Ir multilayers that are analogs of those in several previous reports in which skyrmions are the focus¹¹⁻¹³. The ferromagnet (FM) is amorphous CoFeB or CoB, originally chosen to try and avoid the problems of skyrmion pinning at grain boundaries. Pt and Ir are chosen because they are expected to give rise to DMI of opposite signs at the top and bottom interface and thus a large net DMI, although this is disputed¹⁴. We measure DMI by fitting an expression for the domain wall energy density¹⁵, for which the inputs are temperature-dependent measurements of the saturation magnetization M_S , the exchange stiffness A , the effective perpendicular anisotropy K_{eff} and the domain period d . The low temperature exchange stiffness is determined by fitting an expression for Bloch's law in a thin film to $M_S(T)$, while the domain period is determined from images of the demagnetized domain pattern obtained by wide-field Kerr microscopy in the temperature range 9-290 K. In the Pt/CoFeB/Ir multilayers that we study, the DMI varies between 1.0-1.8 mJ/m², depending on the temperature, while in the Pt/CoB/Ir multilayers the DMI lies in a narrower range between 0.3-0.5 mJ/m². We find that A , K_u and D all scale close to the theoretically predicted behavior.

II. METHODS

The multilayers that we studied consist of (i) [Pt(2.3 nm)/Co₆₈Fe₂₂B₁₀(0.7 nm)/Ir(0.5 nm)]_n (hereafter referred to as CoFeB) and (ii) [Pt(2.3 nm)/Co₆₈B₃₂(0.8 nm)/Ir(0.5 nm)]_n (CoB) deposited by dc magnetron sputtering on a 3 nm Ta

seed layer on a thermally oxidised Si substrate. Thicknesses are nominal values. A 2.3 nm capping layer of Pt was deposited on top to prevent oxidation. The number of repeats n was varied from 1 to 20 and then the samples were subjected to an ac demagnetizing procedure, yielding a maze domain structure at zero field. Three samples were then selected for further study according to their suitability for DMI measurement: those with a large number of domains in the typical field of view in a wide-field Kerr microscope (approximately $200 \mu\text{m} \times 200 \mu\text{m}$ square), to provide a reasonable statistical estimate of the domain period, but with domains that were still well resolved, no narrower than 400 nm. The samples thereby

selected were CoFeB ($n = 2$) and CoB ($n = 5$ and 7).

The saturation magnetization was measured from SQUID-VSM hysteresis loops in the temperature range 9-290 K, and the exchange stiffness at low temperature was found by fitting a modified version of the Bloch $T^{3/2}$ law for thin films to the normalized SQUID-VSM moment versus temperature data.

For thin films the spin wave spectrum is quantised in the thickness direction which leads to a difference in the temperature dependence of magnetization. Bloch's law can be derived^{16,17} in this case by assuming a continuous spin wave spectrum in-plane but a discrete spectrum in the thickness, resulting in the equation

$$\frac{M_S(T)}{M_S(0)} = 1 + \frac{k_B T}{8\pi t} \frac{1}{A(0)} \sum_{p=0}^{N-1} \ln \left[1 - \exp \left\{ -\frac{g\mu_B}{M_S(0)} \frac{1}{k_B T} \left(M_S(0)B_0 + 2A(0) \left(\frac{p}{(N-1)} \frac{\pi}{a_z} \right)^2 \right) \right\} \right], \quad (1)$$

where $M_S(0)$ is the zero temperature magnetization, k_B is the Boltzmann constant, T is the temperature, t is the thickness of a single FM layer, $A(0)$ is the exchange stiffness at low temperature, N is the number of atomic layers in the thickness t , $g = 2.0023$ is the electron g -factor, B_0 is an applied field which saturates the magnetization (here, $B_0 = 1.5$ T, and a_z is the distance between atomic layers in the z -direction. This differs for different lattice types (simple cubic, bcc, fcc) and orientations but all are based on a cubic lattice parameter $a = 0.355$ nm¹⁸. As the FM layers are amorphous the choice of a_z is somewhat arbitrary; we use values that would correspond to bcc and fcc lattices in the [100] and [111] orientations. Equation 1 implies that $M_S(T)$ does not depend on n , which is indeed what we observe across the range of n .

The value of exchange stiffness in Bloch's law is the zero temperature value. Exchange stiffness decreases with increasing temperature due to renormalisation of the magnon spectrum by the thermal magnons¹⁹. Theory and experiment find an approximate power law scaling of the exchange stiffness with the temperature dependent magnetisation where the exponent depends on the lattice geometry⁷. In our analysis we use $A(T)/A(0) = A(m) \sim m^{1.8}$, in line with theory⁸.

The temperature dependence of the magnetic anisotropy field H_K was measured from in-plane SQUID-VSM hysteresis loops. From this we calculate the effective perpendicular anisotropy $K_{\text{eff}}(T) = \frac{1}{2}H_K(T)\mu_0 M_S(T)$. The intrinsic perpendicular anisotropy $K_u(T)$ is then calculated by accounting for the shape anisotropy for a thin film $K_{\text{eff}}(T) = K_u(T) - \frac{1}{2}\mu_0 (M_S(T))^2$ where μ_0 is the vacuum permeability.

In principle $K_u(T)$ contains both bulk magneto-crystalline anisotropies and interface anisotropies. However, for amorphous transition metal films we expect the bulk anisotropy to be negligible. The main source of anisotropy is a two-ion anisotropy at the interfaces, for example Pt-Co where the spin-orbit coupling of the Pt leads to an anisotropic exchange favouring an out of plane orientation for the mag-

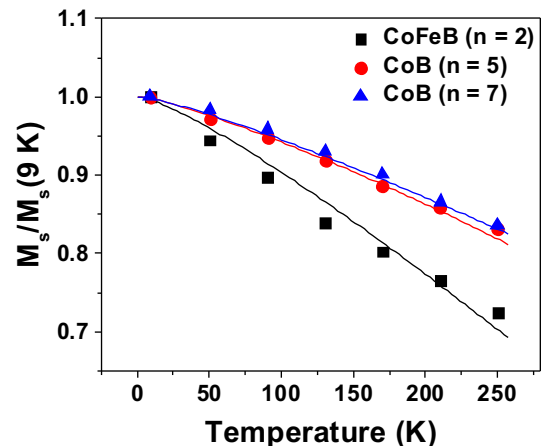


FIG. 1. $M_S(T)$ for [Pt(2.3 nm)/Co₆₈Fe₂₂B₁₀(0.7 nm)/Ir(0.5 nm)]_{n=2} and [Pt(2.3 nm)/Co₆₈B₃₂(0.8 nm)/Ir(0.5 nm)]_{n=5,7}, normalized to the low temperature value. The solid lines are fits to the data using Eq.(1).

netisation. The scaling of two-ion anisotropies according to Callen-Callen theory^{4,5} is $K_u \sim m^2$.

We measured the magnetic domain period in the temperature range 9-290 K from images of the demagnetized domain pattern obtained by wide-field Kerr microscopy. We first saturated the samples in sufficient out-of-plane field (30-50 mT) and then demagnetized them at room temperature by applying a sinusoidally varying out-of-plane field at 0.5 Hz decaying over 120 seconds from a maximum amplitude of 30 mT down to zero. We then mounted each sample in turn in an optical cryostat, cooled to 9 K, and captured an image of the domain pattern at several set temperatures while warming back up to room temperature. Using a similar method to Agrawal et al.²⁰ we extracted the domain period from these images. Briefly: a

TABLE I. Extracted low temperature values of magnetic parameters for the three measured thin films.

	$M_S(9K)$ (MA/m)	$A(9K)$ (pJ/m)	$K_{\text{eff}}(9K)$ (MJ/m ³)	$K_u(9K)$ (MJ/m ³)	$D(9K)$ (mJ/m ²)
CoFeB ($n = 2$)	1.36 ± 0.07	5.5 ± 1.7	1.01 ± 0.08	2.18 ± 0.13	1.8 ± 0.5
CoB ($n = 5$)	1.25 ± 0.04	7.3 ± 1.7	0.80 ± 0.04	1.78 ± 0.08	0.47 ± 0.40
CoB ($n = 7$)	1.26 ± 0.05	7.5 ± 1.8	0.32 ± 0.01	1.32 ± 0.08	0.52 ± 0.31

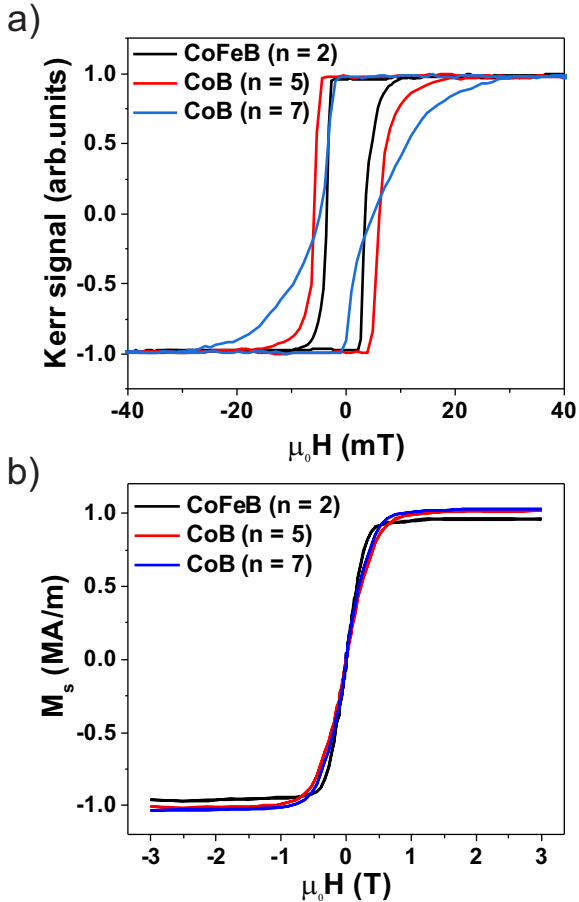


FIG. 2. (a) Hysteresis loops measured at room temperature by magneto-optic Kerr effect with field applied out of plane. (b) Hysteresis loops measured at room temperature by SQUID-VSM with field applied in plane.

fast-Fourier transform of the image produces rings at a characteristic wavelength related to the maze domains. We extracted this wavelength by radially averaging in reciprocal space and fitting a Gaussian function to the intensity. Transforming back into real space the peak of the function gave the average domain period d .

III. RESULTS AND DISCUSSION

Figure 1 shows $M_S(T)/M_S(9K)$ for CoFeB ($n = 2$) and CoB ($n = 5$ and 7) thin films. Fitting the data with Eq. (1)

yields the low temperature value of the exchange stiffness A for each sample, given in Table I. There is a considerable uncertainty in the number of atomic layers represented by the thickness of the film because the film is likely to be rough at the interfaces. We therefore estimated the uncertainty in A by calculating A for $n_z \pm 1$ from the nominal value $n_z = t/a_z$, and taking the largest difference in A as the uncertainty. Our estimated error is therefore large (up to 30%) but we believe it is a realistic estimate of how well A can currently be inferred from thermodynamic measurements in amorphous films. All the values of A here lie within the range of the uncertainty estimated above. We then extrapolated the temperature dependence of A using the power law scaling $A(T)/A(9K) = (M_S(T)/M_S(9K))^{1.8}$ from theory⁸.

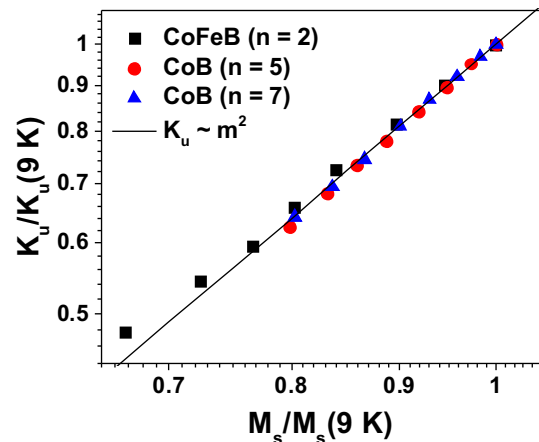


FIG. 3. Log-log plot showing the scaling of the intrinsic perpendicular anisotropy K_u with M_S . The solid line represents the Callen-Callen scaling law $K_u \sim m^2$. Linear fits (not shown) to the data yield the scaling parameters in Table II.

Figure 2 shows hysteresis loops measured at room temperature (290 K) using an out-of-plane field (Figure 2a) and in-plane field (Figure 2b). The former show an expected broadening in the switching field distribution as n increases, due to the increase in interface roughness as successive layers are deposited. The latter were measured as a function of temperature to obtain $H_K(T)$ and thus K_{eff} . The low temperature values of K_{eff} and the intrinsic perpendicular anisotropy K_u are reported in Table I. The uncertainty in the anisotropy is mainly due to the error in measuring the volume of the sample. Figure 3 shows a log-log plot of K_u normalized by the low temperature value plotted against the normalized magnetization. The slope of the linear fit κ ranges from 1.88-2.09 for

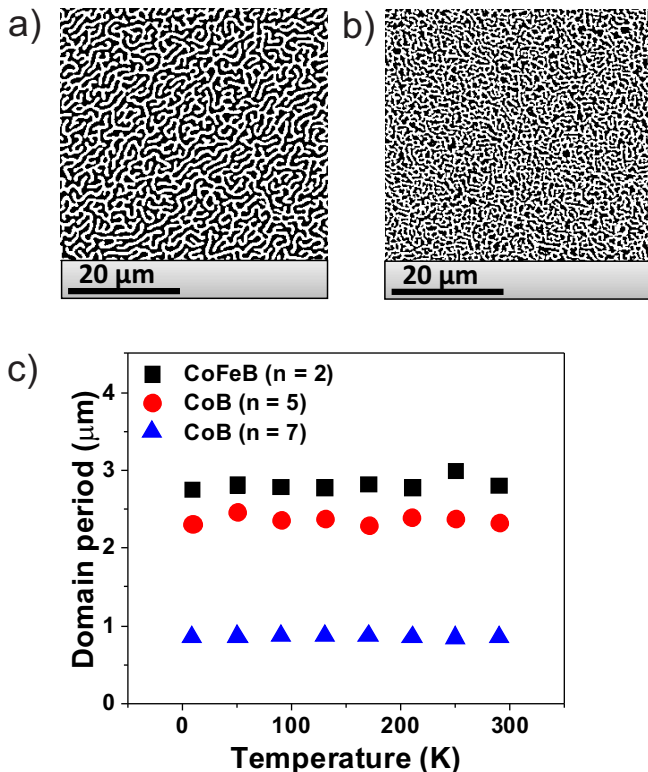


FIG. 4. Demagnetized domain patterns imaged by Kerr microscopy at room temperature for (a) CoFeB ($n = 2$), (b) CoB ($n = 7$). The images have been adjusted to display maximum contrast between up/down domains. (c) Domain period vs. temperature for all three samples. Error bars are smaller than the data points.

TABLE II. Scaling exponents of the magnetic parameters for the three measured thin films. * denotes theoretical value.

	α	κ	δ
CoFeB ($n = 2$)	1.8*	1.88 ± 0.03	1.65 ± 0.04
CoB ($n = 5$)	1.8*	2.09 ± 0.02	1.81 ± 0.09
CoB ($n = 7$)	1.8*	2.05 ± 0.02	1.86 ± 0.05

the different thin films, consistent with a power law scaling of $K_u \sim m^2$ for a two-ion interfacial anisotropy. Table II lists the scaling parameters.

Figure 4 shows typical demagnetized domain patterns at room temperature and the extracted domain period $d(T)$ as a function of the temperature. The domain period does not change with the temperature. For each temperature we use $d(T)$, $M_S(T)$, $A(T)$ and $K_{\text{eff}}(T)$ and calculate the domain wall energy density (in J/m^2)²¹:

$$\sigma_{\text{DW}}(T) = \frac{\mu_0(M_S(T))^2 f d(T)^2}{n\tilde{t}} \times \sum_{\substack{k=1 \\ k \text{ odd}}}^{\infty} \frac{1}{(\pi k)^3} \left[1 - \left(1 + \frac{2k\pi n\tilde{t}}{d(T)} \right) \exp\left(\frac{-2k\pi n\tilde{t}}{d(T)}\right) \right], \quad (2)$$

where f is the magnetic volume ratio of the full stack, and \tilde{t} is the thickness of one Pt/FM/Ir unit in the uniform medium approximation¹⁵. Here, $f = 0.2$ or 0.22 , and $\tilde{t} = 3.5$ nm or 3.6 nm based on the nominal layer thicknesses in the CoFeB and CoB samples, respectively. We find D from the theoretical domain wall energy density²:

$$\sigma_{\text{DW}}(T) = 4\sqrt{A(T)K_{\text{eff}}(T)} - \pi|D(T)|. \quad (3)$$

This analysis yields $D(T)$ for each sample (Figure 5(a)). The uncertainty in A dominates the uncertainty in D . D for both CoB samples is the same within error, as expected, because the interfaces are the same and the only difference is the number of repeats n . The DMI of the CoFeB sample is larger than that of the CoB samples (Table I), which we can ascribe to the presence of Fe and also the smaller atomic percentage of B in the CoFeB sample. The DMI in the CoB samples is in the range of what might be expected given a previous measurement in a $[\text{Pt}(1.0 \text{ nm})/\text{Co}_{80}\text{B}_{20}(0.7 \text{ nm})/\text{Ir}(1.0 \text{ nm})]_{n=6}$

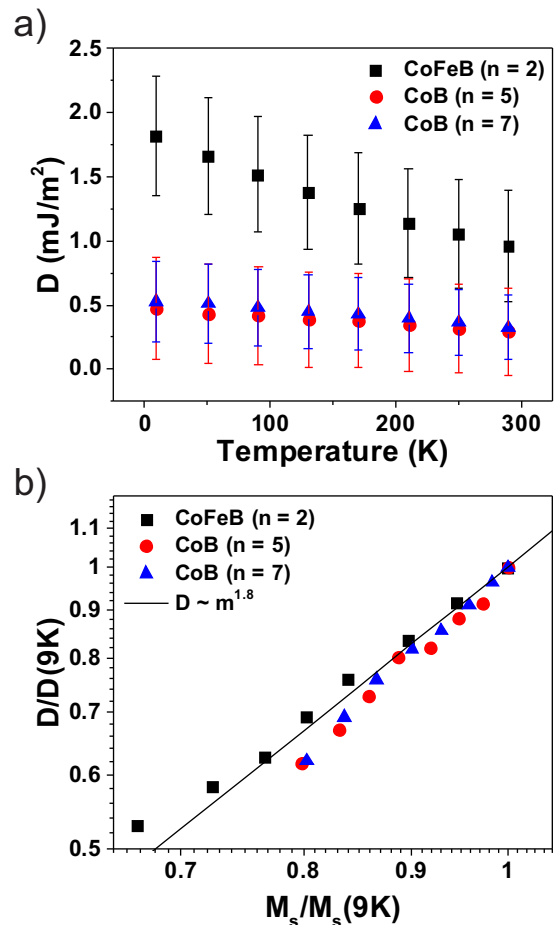


FIG. 5. (a) DMI constant vs. temperature for $[\text{Pt}(2.3 \text{ nm}) / \text{Co}_{68}\text{Fe}_{22}\text{B}_{10}(0.7 \text{ nm}) / \text{Ir}(0.5 \text{ nm})]_{n=2}$ and $[\text{Pt}(2.3 \text{ nm}) / \text{Co}_{68}\text{B}_{32}(0.8 \text{ nm}) / \text{Ir}(0.5 \text{ nm})]_{n=5,7}$. (b) Log-log plot showing the scaling of D with M_S , normalized by the low temperature values. The solid line represents $D \sim m^{1.8}$. Linear fits (not shown) to the data yield the scaling parameters in Table II.

multilayer²². In relative terms, the temperature dependence of the DMI for the CoFeB and CoB samples is the same. Figure 5(b) shows log-log plots of $D(T)$ normalized by the low temperature value against the normalized magnetization. Linear fits yield the scaling exponents, which range from 1.65–1.86 (Table II). The values of the scaling are nearly all the same within error. The scaling for CoFeB ($n = 2$) is only less than that for CoB samples because the data is skewed by one point at room temperature. The scaling parameters are close to the exchange stiffness scaling ~ 1.8 , and align with previous predictions and results^{10,16}. The similar scaling of A and D explains why the domain period is almost independent of temperature. Furthermore, if different values for the scaling of A are used in the analysis (a reasonable range is 1.5–2.0), the scaling of D is the same within the uncertainty of the measurement, i.e. $\alpha = \delta$, a result consistent with numerical simulations^{6–8}.

IV. SUMMARY

We have measured the temperature dependence of the magnetization, perpendicular anisotropy and demagnetized domain period in Pt/CoFeB/Ir and Pt/CoB/Ir multilayers. The domain period does not change significantly as the temperature is varied from 9–290 K. This result can only be obtained if A and D have the same temperature dependence, as predicted by theory. Assuming a scaling of $A \sim m^{1.8}$, we find that, approximately, $D \sim m^{1.8}$, and we report values for the DMI in these films across the temperature range. Pt/CoFeB/Ir exhibits a larger DMI than Pt/CoB/Ir, which we ascribe to the presence of Fe and the smaller at% of B in the former.

V. ACKNOWLEDGEMENTS

K.A. is supported by Jouf University and J.B. by a Royal Society University Research Fellowship. We acknowledge funding from EPSRC grants nos. EP/T006803/1 and EP/T034343/1. We also acknowledge the Exeter Time-Resolved Magnetism Facility (EXTREMAG - EPSRC Grant Reference EP/R008809/1) for variable temperature, wide-field Kerr microscopy. Data associated with this work are available from the Research Data Leeds repository.

-
- ¹ A. Fert and Peter M. Levy, “Role of Anisotropic Exchange Interactions in Determining the Properties of Spin-Glasses,” *Phys. Rev. Lett.* **44**, 1538–1541 (1980).
 - ² André Thiaville, Stanislas Rohart, Émilie Jué, Vincent Cros, and Albert Fert, “Dynamics of Dzyaloshinskii domain walls in ultrathin magnetic films,” *Europhysics Lett.* **100**, 57002 (2012).
 - ³ K. Everschor-Sitte, J. Masell, R. M. Reeve, and M. Kläui, “Perspective: Magnetic skyrmions—Overview of recent progress in an active research field,” *J. Appl. Phys.* **124**, 240901 (2018).
 - ⁴ H.B. Callen and E. Callen, “The present status of the temperature dependence of magnetocrystalline anisotropy, and the $l(l+1)/2$ power law,” *J. Phys. Chem. Solids* **27**, 1271–1285 (1966).
 - ⁵ E.C. Callen and H.B. Callen, “Magnetostriction, Forced Magnetostriction, and Anomalous Thermal Expansion in Ferromagnets,” *Phys. Rev.* **139**, A455–A471 (1965).
 - ⁶ U. Atxitia, D. Hinzke, O. Chubykalo-Fesenko, U. Nowak, H. Kachkachi, O. N. Mryasov, R. F. Evans, and R. W. Chantrell, “Multiscale modeling of magnetic materials: Temperature dependence of the exchange stiffness,” *Phys. Rev. B* **82**, 134440 (2010).
 - ⁷ R. Bastardis, U. Atxitia, O. Chubykalo-Fesenko, and H. Kachkachi, “Unified decoupling scheme for exchange and anisotropy contributions and temperature-dependent spectral properties of anisotropic spin systems,” *Phys. Rev. B* **86**, 094415 (2012).
 - ⁸ R. Moreno, R. F. L. Evans, S. Khmelevskiy, M. C. Muñoz, R. W. Chantrell, and O. Chubykalo-Fesenko, “Temperature-dependent exchange stiffness and domain wall width in Co,” *Phys. Rev. B* **94**, 104433 (2016).
 - ⁹ Sarah Schlotter, Parnika Agrawal, and Geoffrey S. D. Beach, “Temperature dependence of the Dzyaloshinskii-Moriya interaction in Pt/Co/Cu thin film heterostructures,” *Appl. Phys. Lett.* **113**, 092402 (2018).
 - ¹⁰ Yifan Zhou, Rhodri Mansell, Sergio Valencia, Florian Kronast, and Sebastiaan van Dijken, “Temperature dependence of the Dzyaloshinskii-Moriya interaction in ultrathin films,” *Phys. Rev. B* **101**, 054433 (2020).
 - ¹¹ C. Moreau-Luchaire, C. Moutafis, N. Reyren, J. Sampaio, C. A. F. Vaz, N. Van Horne, K. Bouzehouane, K. Garcia, C. Deranlot, P. Warnicke, P. Wohlhüter, J.-M. George, M. Weigand, J. Raabe, V. Cros, and A. Fert, “Additive interfacial chiral interaction in multilayers for stabilization of small individual skyrmions at room temperature,” *Nat. Nanotechnol.* **11**, 444–448 (2016).
 - ¹² Katharina Zeissler, Simone Finizio, Kowsar Shahbazi, Jamie Massey, Fatma Al Ma’Mari, David M. Bracher, Armin Kleibert, Mark C. Rosamond, Edmund H. Linfield, Thomas A. Moore, Jörg Raabe, Gavin Burnell, and Christopher H. Marrows, “Discrete Hall resistivity contribution from Néel skyrmions in multilayer nanodiscs,” *Nat. Nanotechnol.* **13**, 1161–1166 (2018).
 - ¹³ Katharina Zeissler, Simone Finizio, Craig Barton, Alexandra J. Huxtable, Jamie Massey, Jörg Raabe, Alexandr V. Sadovnikov, Sergey A. Nikitov, Richard Brearton, Thorsten Hesjedal, Gerrit van der Laan, Mark C. Rosamond, Edmund H. Linfield, Gavin Burnell, and Christopher H. Marrows, “Diameter-independent skyrmion Hall angle observed in chiral magnetic multilayers,” *Nat. Commun.* **11**, 428 (2020).
 - ¹⁴ Kowsar Shahbazi, Joo-Von Kim, Hans T. Nembach, Justin M. Shaw, Andreas Bischof, Marta D. Russell, Vincent Jeudy, Thomas A. Moore, and Christopher H. Marrows, “Domain-wall motion and interfacial Dzyaloshinskii-Moriya interactions in Pt/Co/Ir(t_{Ir})/Ta multilayers,” *Phys. Rev. B* **99**, 094409 (2019).
 - ¹⁵ Seonghoon Woo, Kai Litzius, Benjamin Krüger, Mi-Young Im, Lucas Caretta, Kornel Richter, Maxwell Mann, Andrea Krone, Robert M. Reeve, Markus Weigand, Parnika Agrawal, Ivan Lemesch, Mohamad-Assaad Mawass, Peter Fis-

- cher, Mathias Kläui, and Geoffrey S. D. Beach, “Observation of room-temperature magnetic skyrmions and their current-driven dynamics in ultrathin metallic ferromagnets,” *Nat. Mater.* **15**, 501–506 (2016).
- ¹⁶ Hans T. Nembach, Justin M. Shaw, Mathias Weiler, Emilie Jué, and Thomas J. Silva, “Linear relation between Heisenberg exchange and interfacial Dzyaloshinskii–Moriya interaction in metal films,” *Nat. Phys.* **11**, 825–829 (2015).
- ¹⁷ Jamileh Beik Mohammadi, Bartek Kardasz, Georg Wolf, Yizhang Chen, Mustafa Pinarbasi, and Andrew D. Kent, “Reduced Exchange Interactions in Magnetic Tunnel Junction Free Layers with Insertion Layers,” *ACS Appl. Electron. Mater.* **1**, 2025–2029 (2019).
- ¹⁸ K. Zeissler, M. Mruczkiewicz, S. Finizio, J. Raabe, P.M. Shepley, A.V. Sadovnikov, S.A. Nikitov, K. Fallon, S. McFadzean, S. McVitie, T.A. Moore, G. Burnell, and C.H. Marrows, “Pinning and hysteresis in the field dependent diameter evolution of skyrmions in Pt/Co/Ir superlattice stacks,” *Sci. Rep.* **7**, 15125 (2017).
- ¹⁹ Charles Kittel, *Quantum Theory of Solids*, 2nd ed. (John Wiley & Sons, 1987).
- ²⁰ Parnika Agrawal, Felix Büttner, Ivan Limesh, Sarah Schlotter, and Geoffrey S. D. Beach, “Measurement of interfacial Dzyaloshinskii–Moriya interaction from static domain imaging,” *Phys. Rev. B* **100**, 104430 (2019).
- ²¹ Ivan Limesh, Felix Büttner, and Geoffrey S. D. Beach, “Accurate model of the stripe domain phase of perpendicularly magnetized multilayers,” *Phys. Rev. B* **95**, 174423 (2017).
- ²² Juriaan Lucassen, Mariëlle J. Meijer, Oleg Kurnosikov, Henk J. M. Swagten, Bert Koopmans, Reinoud Lavrijsen, Fabian Kloudt-Twesten, Robert Frömter, and Rembert A. Duine, “Tuning Magnetic Chirality by Dipolar Interactions,” *Phys. Rev. Lett.* **123**, 157201 (2019).